RANDOM WALK MODELS FOR GEOMETRY-DRIVEN IMAGE SUPER-RESOLUTION

R. Fablet, B.Boussidi

Télécom Bretagne ; UMR LabSTICC
Technopôle Brest-Iroise
29238 Brest cedex, France

E. Autret, B. Chapron

Ifremer/LOS
Technopôle Brest-Iroise
29238 Brest cedex, France

ABSTRACT

This paper addresses stochastic geometry-driven image models and its application to super-resolution issues. Whereas most stochastic image models rely on some priors on the distribution of grey-level configurations (e.g., patch-based models, Markov priors, multiplicative cascades,...), we here focus on geometric priors. We aim at simulating texture samples while controlling high-resolution geometrical features. In this respect, we introduce a stochastic model for texture orientation fields stated as a 2D Orstein-Uhlenbeck process. We show that this process resorts in the stationary case to priors on orientation statistics. We exploit this model to state image super-resolution as a geometry-driven variational minimization, where the geometry is sampled from the proposed conditional 2D Orstein-Uhlenbeck process. We demonstrate the relevance of this approach for real images associated with the remote sensing of ocean surface dynamics.

***Index Terms*—** texture geometry, orientation field, stochastic models, Ornstein-Uhlenbeck process

1. PROBLEM STATEMENT AND RELATED WORK

Texture analysis and modeling have been over the last decades extremely active research topics. One may cite a variety of models and approaches including Markov models, patch-based/exemplar-based schemes, multiplicative cascades, marginal-based models,... e.g. [4, 7, 11, 13]. Impressive applications to texture synthesis have been reported, especially using example-based/patch-based techniques [7, 11]. More recently, image super-resolution has also emerged as hot topic [3, 9, 10, 11, 12], including texture-based super-resolution [3, 5, 10, 11].

A common feature shared by these models is that they state some explicit (e.g., Markov, AR and cascade models) or implicit (e.g., patch-based schemes) priors on a 2D scalar field which represents the processed image. It is well-known that geometry and contrast are potentially independent features that may be addressed separately, in the sense that a given texture geometry remains unchanged whatever the contrast function [15]. However to our knowledge none of these models explicitly consider priors on the geometry of texture samples. Multiplicative cascades as well as other fractal models [4] only partially address such geometrical priors as the fractal dimension and/or multifractal spectrum typically depends both on the image geometry and on the local contrast.

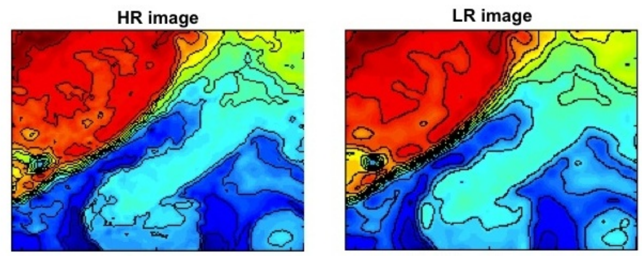

Fig. 1. **Geometry-driven super-resolution:** we aim at simulating a high-resolution (HR) textured image given a low-resolution (LR) image based on geometric priors. The LR image is a downsampled version of the HR image.

Our work aims at proposing such stochastic geometry-driven priors for image modeling and synthesis. This approach is also motivated by studies which stress the relevance of the geometrical component of visual textures for segmentation and recognition issues, for instance using point processes [16] or texture orientation statistics [17]. In this work, we further explore texture geometry and the definition of stochastic geometry-driven image models. Regarding image level-lines as the realizations of correlated random walks (Orstein-Uhlenbeck process), image orientation fields are stated as realizations of 2D Orstein-Uhlenbeck processes. This model which embeds priors on orientation statistics is applied to image super-resolution as illustrated in Fig.1. To our knowledge, the proposed stochastic model is the first one to explicitly consider priors on the geometry of texture level-lines for simulation and super-resolution applications.

2. STOCHASTIC GEOMETRY IN IMAGES

The geometry of grey-level or scalar images is fully characterized by the geometry of their level-lines [15]. The associated contrast-invariant representation has been exploited in a number of applications such as inpainting, coding as well as texture recognition [1, 18]. For some classes of textured images, such as image of turbulent dynamics, several theoretical and experimental studies have specifically explored the statistical features which characterize the geometry of the image level-lines [1, 2]. We here further explore the extent to which image level-lines may be regarded as random walk samples.

2.1. Image level-lines as 2D random walks

We propose to model image level-lines as constant-velocity 2D random walks defined by a Orstein-Ulhenbeck process [6]:

$$d\theta(t) = -\gamma\left(\theta(t) - \theta_0\right)dt + \sigma dW(t) \tag{1}$$

where $\theta(t)$ is the direction of the displacement at time t. θ_0 is a directional bias. $dW(t)$ is a 1D brownian process. γ and σ are positive scalar parameters. The first term is a linear reorientation model which states the directional drift of the random walk. This reference direction is introduced here as a constant for the sake of simplicity. In a second step, it may vary to account for a coarse-scale geometric prior. It may also be noted that other reorientation models, such as sinusoidal ones, could be considered [6]. From (Eq.1) the sampling of the random walk for a discretization time step Δt follows as:

$$\begin{aligned} \theta(t_0 + k\Delta t) &= \alpha\left[\theta_0 + \frac{\sigma}{\gamma}\Delta t \tilde{W}(t_0 + k\Delta t)\right] \\ &+ (1-\alpha)\theta(t_0 + (k-1)\Delta t) \end{aligned} \tag{2}$$

where t_0 is the initial time, k the time index, $\alpha = 1 - \exp(-\gamma\Delta t)$ and $\tilde{W}$ a centered and normalized white noise.

The stationary statistics of the considered random walk can be derived from the associated Fokker-Plank equation [6] and this discretization scheme. The stationary distribution of the orientation θ is a wrapped normal distribution with mean θ_0 and variance $\gamma^2\sigma^2$ and the stationary distribution of the turning angle between time instants t and $t + \Delta t$ is a zero-mean wrapped normal distribution with standard deviation $\alpha\Delta t\sigma/\gamma$. Hence, parameters γ and σ clearly control the geometry of the sampled trajectories.

2.2. Stochastic orientation field model

As image level-lines are not mutually independent, the key idea of the proposed stochastic geometry-driven image model is to state the image orientation field as a 2D Orstein-Ulhenbeck process such that each level-line is characterized by a random walk model similar to (Eq.1). Let us denote by $\theta(p)$ the local orientation at pixel location p. We consider the following 2D Orstein-Ulhenbeck process:

$$d\theta(p) = -\gamma\left(\theta(p) - \theta_0(p)\right)dp + \sigma dW(p) \tag{3}$$

where W is 2D Brownian surface. Parameters γ and σ have the same interpretation as in Eq. 1. It should be noted that this model guarantees that the orientation along the level-line, which corresponds to the projection of Eq.(3) onto the tangent $(\cos\theta(t) \quad \sin\theta(t))^t$ to the image level-line at point p, verifies a stochastic equation similar to Eq. 1. This property relates the geometric features of the level-lines to the orientation statistics of the random field θ.

2.3. Stochastic geometry-driven texture model

Based on the stochastic orientation field model, we define a geometry-driven texture model such that texture samples $\tilde{I}$ are sampled according to:

$$\left\{\begin{array}{l} d\theta(p) = -\gamma\left(\theta(p) - \theta_0(p)\right)dp + \sigma dW(p) \\ \\ \langle n_{\tilde{I}}(p), u_\theta(p)\rangle = 0,\ \forall p \end{array}\right. \tag{4}$$

where $n_{\tilde{I}}(p) = \nabla\tilde{I}(p)/\|\nabla\tilde{I}(p)\|$ is the normal to the level-line of image $\tilde{I}$ at point p and $u_\theta(p)$ the unit direction vector $(\cos\theta(t) \quad \sin\theta(t))^t$. This system is turned into the combination of the sampling of the orientation field and of a variational minimization:

$$\left\{\begin{array}{l} d\theta(p) = -\gamma\left(\theta(p) - \theta_0(p)\right)dp + \sigma dW(p) \\ \\ \tilde{I} = \arg\min\limits_I \int \|\langle\nabla I(p), u_\theta(p)\rangle\| dp \end{array}\right. \tag{5}$$

The stochastic simulation of images involves two steps:

1. *the generation of a sample of the orientation field model* θ: the integration of the stochastic differential equation (5) proceeds according to a lexicographical scan of the image. At each point, we randomly select the horizontal or vertical direction and consider the integration (2) according to the selected direction.

2. *the computation of the image sample* $\tilde{I}$ *from the minimization of the proposed variational cost*: We solve for this minimization using an iterated reweighted least square (IRLS) scheme applied to a discretized version of the variational cost from an initial image $\tilde{I}^0$. This IRLS scheme is similar to the one detailed in [8].

2.4. Model simulations

We illustrate simulations for two different parameter settings for γ and σ (Fig.2) using a constant reference orientation $\theta_0 = \pi/2$ and the same initialization $\tilde{I}^0$ (Fig.2, upper-left). Whereas along-level-line orientation statistics are similar (Fig.2, left row, bottom panel), the global geometric patterns strongly differ. It might be noted that the sampled images correctly match to the theoretical stationary statistics.

A textured image typically involves these different types of geometries, that is to say both areas depicting regular level-lines and areas involving irregular ones. Varying spatially model parameters σ and γ, our model can represent and model the geometric variabilities of a textured image with respect to a reference geometry θ_0.

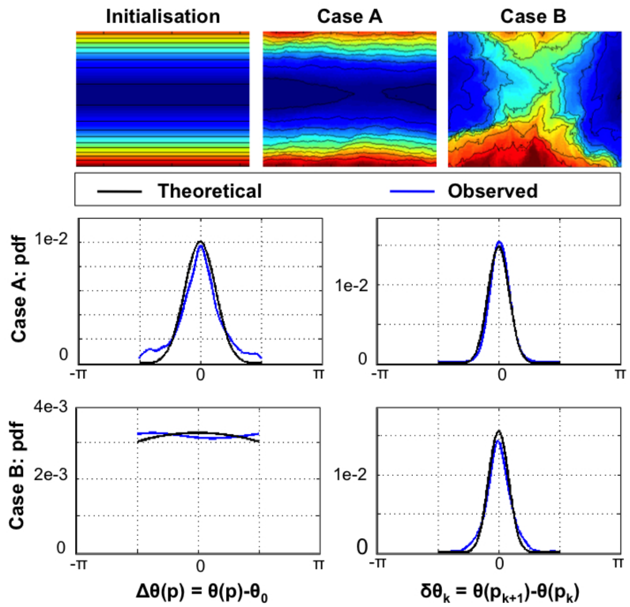

Fig. 2. Simulations of the stochastic image model (Eq.5) in the stationary case: first row, considered initialisation (left), simulation for parameter setting A (center), simulation for parameter setting B (right); second row, orientation varibility w.r.t. the directional drift (left) and along-level-line turning angle statistics (right) for parameter setting A; third row, the same as the second row for parameter setting B. Observed orientation statistics (blue,-) are compared to theoretical stationary statistics (black,-). The considered parameter settings are as follows: $\gamma = 0.6$ and $\sigma = 0.3$ for case A, and $\gamma = 5e-3$ and $\sigma = 0.4$ for case B.

3. APPLICATION TO IMAGE SUPER-RESOLUTION

As an application of the proposed stochastic image model, we consider the super-resolution of textured images. We aim at simulating a high-resolution textured image given a low-resolution sample (Fig.1). Our specific interest is in the statement of a geometry-driven prior to constrain the geometry of the high-resolution image conditionally to the low-resolution observation. We first describe the proposed super-resolution model and the associated numerical implementation. In a second step we present experiments on real images.

3.1. Stochastic super-resolution model

To state our model, we introduce the following notations. Let I_{HR} be a $N \times M$ high-resolution scalar image and I_{HR} its low-resolution counterpart. We assume that I_{LR} is a K^{th}-order subsampled version of I_{HR}, where $\mathcal{P}$ is the projection operator of the subsampling process: $I_{LR} = \mathcal{P}[I_{HR}]$ and by $\mathcal{P}^{-1}$ the interpolation operator from a $N/K \times M/K$ resolution to a $N \times M$ one. $\mathcal{P}$ satisfies an orthogonality constraint:

$$I_{LR} = \mathcal{P}\left[\mathcal{P}^{-1}[I_{LR}]\right] \quad \text{and} \quad \mathcal{P}[I_{HR} - \mathcal{P}[I_{HR}]] = 0 \quad (6)$$

Formally the super-resolution issue is stated as the sampling of a stochastic model conditionally to a low-resolution observation I_{LR}:

$$\text{sample } I|I_{LR} \text{ subject to } I_{LR} = \mathcal{P}[I] \quad (7)$$

The stochastic model proposed in the previous section (Eq.5) naturally applies to consider geometry-driven priors in the definition of the conditional distribution $P(I|I_{LR})$ and the geometry-driven super-resolution model resorts to:

$$\begin{cases} d\theta(p) = -\gamma(p)\left(\theta(p) - \theta_{LR}(p)\right)dp + \sigma(p)dW(p) \\ \tilde{I} = \arg\min_{I} \int \|\langle \nabla I(p), u_\theta(p)\rangle\| dp \\ \text{Subject to } I_{LR} = \mathcal{P}\left[\tilde{I}\right] \end{cases} \quad (8)$$

where W is a Brownian surface, θ_{LR} the orientation field of the tangent to the level-lines, *i.e* $(-\sin\theta_{LR} \quad \cos\theta_{LR})^t = \nabla I_{LR}/\|\nabla I_{LR}\|$ with ∇I_{LR} the gradient of image I_{LR}.

This stochastic super-resolution clearly constrains the geometry of the high-resolution sample $\tilde{I}$ from the geometry of the low-resolution image through orientation field θ_{LR}. Model parameters γ and σ may here spatially vary to account for the non-stationarity of the geometry of the image. These parameter fields are defined according to the following statement: level-lines corresponding to image contours typically depict greater geometrical regularity than level-lines in flat image regions. We then use the magnitude of the image gradient as a local cue on the regularity of the level-lines, and we parameterize fields γ and σ as follows:

$$\begin{cases} \gamma(p) = \gamma_0 \|\nabla I_{LR}(p)\|^{\nu} \\ \sigma(p) = \sigma_0 \|\nabla I_{LR}(p)\|^{-\beta} \end{cases} \quad (9)$$

where γ_0, σ_0, ν and β are positive scalar parameters. The greater the magnitude of the low-resolution gradient, the greater parameter γ, such that the re-orientation term in the local variations of θ (Eq.2) becomes stricter. By contrast, the lower the magnitude of the low-resolution gradient, the greater parameter σ and the relative weight of the Brownian surface. Hence for very large gradients, the local orientation is constrained to that of the low-resolution observation, whereas in uniform areas only the Brownian process, independent on the low-resolution condition, is active.

3.2. Numerical resolution

The proposed stochastic super-resolution model involves two steps: the generation of a sample of the orientation field model and the resolution of the geometry-driven variational minimization. The first step is similar to the procedure described previously for the model with constant parameters (Eq.5). Regarding the variational minimization, we proceed as follows to fulfill projection constraint $I_{LR} = \mathcal{P}[I]$.

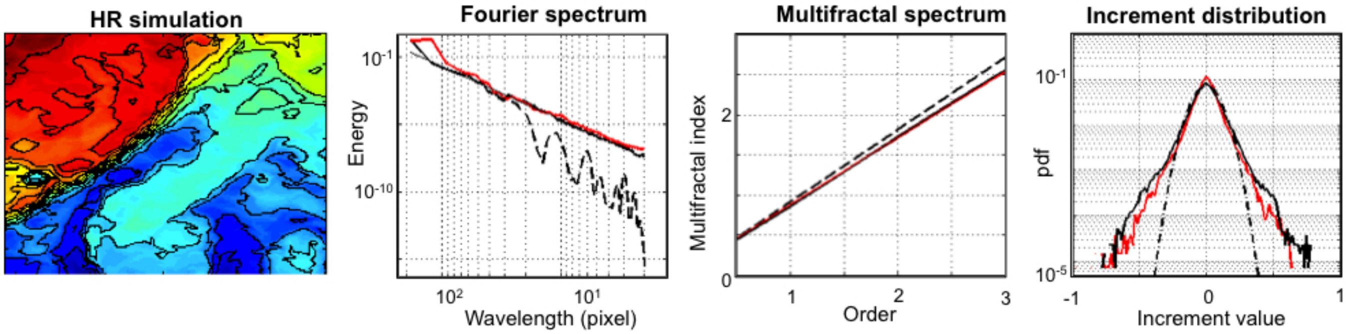

Fig. 3. Stochastic geometry-driven super-resolution of real images: from left to right, simulated high-resolution image given the low-resolution image depicted in Fig.1, Fourier spectrum of the simulated image (red,-) compared to the Fourier spectra of the real high-resolution (black, -) and low-resolution (black,–) images depicted in Fig.1, multifractal spectrum of the the simulated image (red,-) compared to the multifractal spectra compared to the Fourier spectra of the real high-resolution (black, -) and low-resolution (black,–) images, comparison of the distribution of fine-scale details $I - I_{LR}$ of the simulated image (red, -) to the distribution of fine-scale details $I_{HR} - I_{LR}$. The latter also depicts a normal distribution with the same variance as $I - I_{LR}$ to check for the non-gausssianity of the fine-scale details.

The considered IRLS scheme iteratively updates the solution from the initialization $\tilde{I}^{(0} = \mathcal{P}^{-1}[I_{LR}]$. Let us denote by $\delta\tilde{I}^{(k)}$ the incremental update at iteration $k$such that $\tilde{I}^{(k+1)} = \tilde{I}^{(k)} + \delta\tilde{I}^{(k)}$ with $\tilde{I}^{(k)}$ the solution at iteration k. To fulfiil the projection constraint, we exploit the orthogonality of projection operator $\mathcal{P}$ and we modify the update to $\tilde{I}^{(k+1)} = \tilde{I}^{(k)} + \delta\tilde{I}^{(k)} - \mathcal{P}\delta\tilde{I}^{(k)}$ such that $\tilde{I}^{(k+1)}$ verifies $\mathcal{P}\tilde{I}^{(k+1)} = I_{LR}$.

In our implementation, we consider power-two subsampling factor $K = 2^L$ and we use 2D discrete wavelet transforms [14] such that projection operator $\mathcal{P}$ satisfies (Eq.6). The projection constraint resorts to keeping only the detail coefficients of the discrete transform of the updated image $\tilde{I}^{(k+1)}$ up to level L while approximation coefficients at level L are given by those of the low-resolution observation I_{LR}.

3.3. Experiments

In our experiments, we consider an application to the remote sensing of ocean surface dynamics, especially satellite-based sea surface temperature images (Fig.3). SST images are also known to be intimately linked to the turbulent ocean dynamics and involve complex multiscale cascades as well as geometrical properties [1, 2]. Whereas high-resolution satellite observations (e.g., infrared sensor) are more affected by the cloud cover as well as to rain effects, low-resolution observations (e.g., micro-wave sensor) present lower rate of missing data. The proposed super-resolution algorithms are then of key interest to address missing data interpolation in high-resolution images given the associated low-resolution observation.

The reported example (Fig.3) illustrates the relevance of the proposed stochastic geometry-driven model to generate a high-resolution image visually similar to the real image, especially in terms of geometrical features. The parameter setting is the following: $\nu = 0.54$, $\beta = 0.13$, $\gamma_0 = 2.14$, $\sigma_0 = 0.14$. Our super-resolution scheme also recovers a correct decay in the Fourier spectrum as well as a multifractal spectrum very similar to that of the real image. It should be noted that no explicit constraint is set in our model on the Fourier and multifractal spectra. The good match with the real image is interpreted as a consequence of the multiscale cascades implicitly encoded by the considered stochastic model. We also report the comparison of the distributions of the fine-scale details of the simulation vs. the real image. They clearly outline the non-gaussianity of these details between the two analysis scales for the real image. This property is a widely acknowledged feature of real images [4] and further stresses the the relevance of the proposed stochastic geometry-driven image model to generate non-gaussian surfaces.

4. CONCLUSION

We have presented a novel stochastic image model. Contrary to most probabilistic models of scalar images, the prior is not explicitly set on image values nor responses to filter banks [4, 7, 13], but on the orientation field constraining the geometry of image level-lines. It then allows us to control geometrical features, in terms of local regularity of the level-lines. The stochastic orientation field model is stated as 2D Orstein-Uhlenbeck process. This model naturally applies to texture super-resolution. The simulation of real high-resolution images of the sea surface temperature outline the relevance of the proposed model.

Our future work will further explore the proposed framework. Regarding theoretical aspects, we will focus on the analysis of the stationary distribution of the considered Orstein-Uhlenbeck process as well as extensions to fractional Brownian surfaces. Besides applications to the texture-based interpolation of mission data and spatio-temporal extensions of the proposed model are also of interest.

5. REFERENCES

[1] Ba, S., et al. Statistical descriptors of ocean regimes from the geometric regularity of Sea Surface Temperature observations. *IEEE GRSL*, 2012.

[2] Bernard, D., Boffetta, G., Celani, A., Falkovich, G. Conformal invariance in two-dimensional turbulence. *Nature Physics*, 2(2): 124-128, 2006

[3] Byung Tae Oh, Jay Kuo, C.-C. Super-resolution texture synthesis using stochastic PAR/NL model. *JVCR*, 23(7):995-1007, 2012.

[4] Chainais, P. Infinitely Divisible Cascades to Model the Statistics of Natural Images. *IEEE TPAMI*, 29(12):2105-2119, 2007.

[5] Chainais, P. Kœnig, E., Delouille, V., Hochedez, J.-F. Virtual super resolution of textured images using multifractal stochastic processes. *JMIV*, 39(1):28-44, 2011.

[6] Codling, E.A., Plank, M.J., Benhamou, S. Random walk models in biology. *J. R. Soc. Interface*, 5:813-834, 2008.

[7] Efros, A.A., Freeman, W.T. Image Quilting for Texture Synthesis and Transfer. *Proc. ACM SIGGRAPH*, 2001.

[8] Fablet, R., Pujolle, S., Chessel, A., Benzinou, A., Cao F. 2D Image-based reconstruction of shape deformation of biological structures using a level-set representation. *CVIU* , 111(3):295-306, 2008.

[9] Fattal, R. Image upsampling via imposed edge statistics. *Proc. ACM SIGGRAPH*, 26(3):95-102, 2007.

[10] Freeman, W.T., Jones, T.R., Pasztor, E.C. Example-based super-resolution. *IEEE Comp. Graph. App.*, 22(2):56-65, 2002.

[11] Freeman, W.T., Liu, C. Markov Random Fields for Super-resolution and Texture Synthesis. *In A. Blake, P. Kohli, and C. Rother, eds., Advances in Markov Random Fields for Vision and Image Processing*, Chapter 10. MIT Press, 2011.

[12] Glasner, D., Bagon, S., Irani, M. Super-resolution from a single image. *Proc. ICCV*, 2009.

[13] Heeger, D.J., Bergen, J.R. Pyramid Based Texture Analysis/Synthesis. *Proc. ACM SIGGRAPH*, 229-238, 1995.

[14] Mallat, S. (2008). A Wavelet Tour of Signal Processing. Academic Press.

[15] Monasse, P., Guichard, F. Fast Computation of a Contrast Invariant Image Representation. *IEEE TIP*, 9:860-872, 2000.

[16] Nguyen, H.-G., Fablet, R., Boucher J.M.. Keypoint-based analysis of sonar images: application to seabed recognition. *IEEE TGRS*, to appear, 2012.

[17] Varma, M., Zisserman, A. A statistical approach to texture classification from single images. *IJCV*, 62(1–2):61-81, 2005.

[18] Xia, G.-S., Delon, J. , Gousseau, Y. Shape-based invariant texture indexing. IJCV, 88(3):382-403, 2010.